Chemistry
A European
Journal

Chemistry Europe
European Chemical Societies Publishing

Accepted Article

Title: Anthraquinone-Modified Silica Nanoparticles as Heterogeneous Photocatalyst for the Oxidative Hydroxylation of Arylboronic Acids

Authors: María Guadalupe Martin, Juan Manuel Lázaro-Martínez, Sandra Elizabeth Martín, Paula Marina Uberman, and María Eugenia Budén

To be cited as: *Chem. Eur. J.* **2023**, e202303382

Link to VoR: https://doi.org/10.1002/chem.202303382

WILEY VCH

10.1002/chem.202303382

WILEY VCH

RESEARCH ARTICLE

Anthraquinone-Modified Silica Nanoparticles as Heterogeneous Photocatalyst for the Oxidative Hydroxylation of Arylboronic Acids

María Guadalupe Martin,[a],[b] Juan Manuel Lázaro-Martínez,[c],[d] Sandra Elizabeth Martín,[a],[b] Paula Marina Uberman,[a],[b]* and María Eugenia Budén[a],[b]*

Dedicated to Emeritus Professor Roberto Arturo Rossi on the occasion of his 80th birthday celebration

Eng. M. Guadalupe Martin, Dr. Juan Manuel Lázaro-Martínez, Prof. Sandra E. Martín, Prof. Paula M. Uberman, Prof. María E. Budén

[a] Departamento de Química Orgánica, Facultad de Ciencias Químicas, Universidad Nacional de Córdoba

[b] Instituto de Investigaciones en Fisicoquímica de Córdoba-INFIQC-CONICET-Universidad Nacional de Córdoba
Address: Haya de La Torre y Medina Allende, Ciudad Universitaria, X5000HUA, Córdoba, Argentina
E-mail: paula.uberman@unc.edu.ar; eugebuden@unc.edu.ar

[c] Departamento de Ciencias Químicas, Facultad de Farmacia y Bioquímica, Universidad de Buenos Aires

[d] Instituto Química y Metabolismo del Fármaco IQUIMEFA-UBA-CONICET
Address: Junín 956, C1113AAD, Ciudad Autónoma de Buenos Aires, Argentina.

Supporting information for this article is given via a link at the end of the document.

Abstract: In this work, the synthesis and characterization of a heterogeneous photocatalyst based on spherical silica nanoparticles superficially modified with anthraquinone 2-carboxylic acid (AQ-COOH) are presented. The nanomaterial was characterized by TEM, SEM, FT-IR, diffuse reflectance, fluorescence, NMR, DLS, XRD and XPS. These analyses confirm the covalent linking of AQ-COOH with the NH_2 functionality in the nanomaterial and, more importantly, the photocatalyst retains its photophysical properties once bound. The heterogeneous photocatalyst was successfully employed in the aerobic hydroxylation of arylboronic acids to phenols under sustainable reaction conditions. Phenols were obtained in high yields (up to 100 %) with low catalyst loading (3.5 mol %), reaching TOF values of 3.7 h^{-1}. Using 2-propanol as solvent at room temperature, the visible light photocatalysis produced H_2O_2 as a key intermediate to promote the aerobic hydroxylation of arylboronic acids. The heterogeneous photocatalyst was reused at least 5 times, without modification of the nanomaterial structure and morphology. This simple heterogeneous system showed great catalytic activity under sustainable reaction conditions.

Introduction

Photoredox reactions comprise an energy-conversion process in which the absorption of photons by a substance triggers an electron transfer process. In the past decade, these reactions have been widely used in organic synthesis mediating chemical reactions to produce pharmaceuticals, fine chemicals and advanced materials.[1] In photoredox reactions, the use of metallic and organic photocatalysts (PCs) is widespread, since they are able to mediate complex reactions with high efficiency and under sustainable reaction conditions. The usefulness of photoredox reactions has been recently demonstrated by mediating reactions that have so far been difficult to accomplish with conventional catalysts. Novel organic transformations were achieved, improving the efficiency and sustainability of synthetic strategies to afford numerous organic compounds.[2] The most commonly used PCs in organic synthesis include organic dyes such as perylene diimides (PDIs) and xanthene derivatives,[3] and organometallic Ir and Ru complexes.[4]

In the past decade, special efforts have been made to improve the use of organic PCs in organic synthesis, particularly in large-scale reactions due to their low cost. Among organic PCs, anthraquinones (AQs) are an important class of organic dyes recently used in visible-light prompted photoredox organic transformations.[5] These organic dyes constitute an abundant family of natural products found in various plants and microorganisms, and they offer broad applications and bioactivities. The efficiency of AQs as PCs is linked to the excited-state reduction potential (E^*_{red} ≈ -0.50 V vs SCE in aprotic solution).[6],[7] A wide number of research of electron-transfer (ET) reactions involving AQs that proceed by simultaneous redox reactions with electron, deuterium, or hydrogen-atom abstraction were reported.[5]

The use of homogeneous PCs presents certain limitations, particularly with regard to challenges in catalyst removal and the photostability of PCs. Therefore, the design of photocatalytic systems that improve the recuperation and reuse of PCs is required in order to increase the use of photoredox catalysis in organic synthesis. One way to improve PC recovery is to prepare heterogeneous PCs.[8],[9] Examples of recyclable heterogeneous photocatalysts (PCs) include the use of mesoporous graphitic carbon nitride (mpg-CN),[10] and metal-organic organic frameworks (MOFs) materials.[11] However, with these materials it is difficult to tune PCs photochemical properties without altering the physical properties of the material. A simpler strategy to prepare heterogeneous PCs, which allows merging the properties of homogeneous and heterogeneous systems, comprises the

10.1002/chem.202303382

immobilization of homogeneous PC with a well-known photochemical activity into an insoluble material by a covalent functionalization.[12] With this strategy, several heterogeneous PCs were developed by incorporating organometallic complexes or small-organic molecules over polymers,[13] titanium dioxide,[14] MOFs,[15] among other materials, reaching excellent results in terms of catalytic efficiency and recyclability of PCs.[16] Recently, the immobilization of AQs was evaluated over several materials like–polymers,[17],[18] MOF,[19], [20] and inorganic materials.[21],[22] Heterogeneous AQ photocatalysts were employed in several reactions, including the cross-dehydrogenative coupling of *N*-aryl tetrahydroisoquinolines,[18] oxidation of benzylic alcohol,[19] among other reactions.

Silicon supports are widely used in heterogeneous catalysis due to their large surface area, excellent chemical stability, and in some cases high porosity. Moreover, silica nanoparticles were used as supports, because they present several advantages such as chemical inertness, transparency, good biocompatibility and easy functionalization of their surface. On account of these properties, silicon-type material can host diverse PCs (e.g., metals and organic dyes),[23], [24], [25], [26], [27], [28] with good anchoring and easy recycling, leading to a large variety of possible chemical reactions.[29]

Among the organic transformations that take place in the presence of PCs, the obtaining of substituted phenols presents important industrial applications. Phenols are used in manufacturing polymers and producing biologically active ingredients with pharmaceutical and agrochemical applications.[30] These important building blocks can be synthesized from arylboronic acids by aerobic photo-oxidation processes.[31] This is a versatile and convenient method for preparing substituted phenols, since it usually employs mild reaction conditions, and phenols are afforded in good yields.[32–34] However, these reactions show some drawbacks like the use of UV light irradiation;[35] the reaction proceeds with sacrificial donors like triethylamine and *N*,*N*-diisopropylethylamine (DIPEA);[36],[37] or with non-sustainable oxidants.[38] For example, recently, Teixeira *et. al.* prepared Ru complexes supported into glass-wool material, which was successfully employed in the oxidative hydroxylation of arylboronic acids to afford phenols, with DIPEA as a donor in MeCN:H_2O mixture, after 6 hours.[25] This PC was reused at least 6 times without any significant loss of activity.

Herein we report the synthesis and characterization of a heterogeneous organic dye PC obtained by immobilization of anthraquinone 2-carboxylic acid (AQ-COOH) onto spherical silica nanoparticles (SNPs) with well-defined size and morphology. The heterogeneous PC synthesis took place under sustainable reaction conditions. The catalytic activity of the heterogeneous PC was evaluated in the oxidative hydroxylation of arylboronic acids as a model reaction. Furthermore, the catalytic activity of the heterogeneous PC was compared with that of the corresponding homogeneous system, and the recovery and reuse of the heterogeneous systems are discussed.

Results and Discussion

Synthesis and characterization of anthraquinone-based heterogeneous photocatalyst

With the aim of preparing heterogeneous anthraquinone-based photocatalysts, the immobilization of anthraquinone 2-carboxylic acid (AQ-COOH, Figure 1), onto SiO_2 nanoparticles (SNPs) was performed.

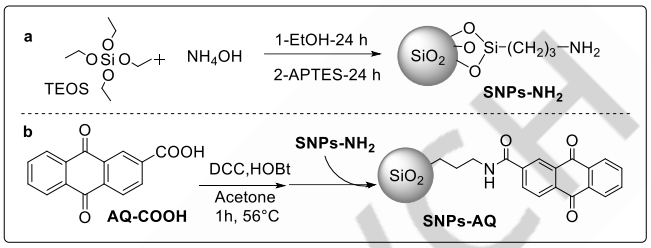

Figure 1. Synthetic methodology to prepare SNPs-AQ photocatalyst.

First, SNPs functionalized with surface amino groups were synthesized by the Stöber method (SNPs-NH_2, Figure 1a).[39] Spherical SNPs were obtained by mixing the proper amounts of TEOS, NH_4OH, and ethanol. Then, in a one-pot procedure, the SNPs were superficially modified by incorporating (3-aminopropyl)-triethoxysilane (APTES) into the ethanolic reaction mixture, to obtain SNPs-NH_2.

This functionalization introduced amino functional groups into the surface of SNPs, essential groups to achieve the immobilization of AQ-COOH by amide bond formation using carbodiimide chemistry. The formation of amide bond was carried out with specific activating reagents for carboxylic acid groups, such as *N*,*N*´-dicyclohexylcarbodiimide (DCC) and 1-hydroxibenzotriazole (HOBt), a widely used combination for the formation of amide bonds.[40] The previously reported methods to perform this reaction usually employed nonpolar solvents, even toxic ones like toluene.[41] Herein, acetone was used as a solvent. Thus, the activation of AQ-COOH was accomplished with DCC and HOBt in acetone at 56 °C for 1 h (Figure 1b). Subsequently, the SNPs-NH_2 were added (in a mass ratio SNPs-NH_2:AQ-COOH 10:1), and the mixture was allowed to react at room temperature for 24 h. The heterogeneous photocatalyst SNPs-AQ was centrifuged, washed, and then dried and stored under air, for subsequent use.

The as-obtained nanomaterials were fully characterized by SEM, TEM, DRX, TGA, UV–vis diffuse reflectance spectroscopy, solid-state fluorescence spectroscopy, UV, FT-IR, *ss*-NMR, XPS and DLS (Figure 2 and Figure SI4-SI9). Consequently, the morphology and size of SNPs-NH_2 and SNPs-AQ were analyzed by TEM and SEM examination. TEM micrographs demonstrated that NPs were spherical with an average diameter of just about 250 nm (Figure 2a-d). SEM analysis showed similar results, observing the formation of dense particles (Figure SI4a-b, Supporting Information). The precursor SNPs-NH_2 presented particles with an average diameter of (256 ± 22) nm (Figure 2a-b). After functionalization with AQ-COOH, the obtained SNPs-AQ exhibited an average diameter of (252 ± 23) nm (Figure 2c-d).

10.1002/chem.202303382

Thus, the functionalization process with AQ-COOH did not significantly modify the size and shape of SNPs.

The XRD pattern exhibited the characteristic diffraction broad peak centered on 24° (2θ), confirmed the amorphous nature of SNPs obtained by Stöber methodology (Figure SI4c).[27] This structure was maintained after PC immobilization, and no other crystalline phase was observed in the XRD pattern. Therefore, solid and spherical SNPs with amorphous structure were obtained by this procedure.

The organic content was determined by thermogravimetric analysis (TGA, Figure 2e). In SNPs-NH_2 particles, two steps of weight reduction were observed. An initial weight loss ranged from 40°C-160°C, essentially caused by water vaporization of the absorbed water. In the second temperature range, between 160°C-600 °C, a higher percentage of weight drop was observed for SNPs-NH_2 compared with SNPs (Figure SI4d), due to the thermal decomposition of the organic aminopropyl coating (almost 3 wt%). The SNPs functionalized with AQ-COOH (SNPs-AQ) exhibited a larger weight loss than SNPs-NH_2, indicating the suitable incorporation of PC over the SNPs. Thus, 3.9 wt % of AQ-COOH in SNPs was determined, representing 0.154 mmol of AQ-COOH per gram of nanomaterial.

The UV–visible diffuse reflectance spectra for SNPs-AQ, AQ-COOH, and a physical mixture of SNPs-NH_2 and AQ-COOH (3.9 wt %) are presented in Figure 2f. After PC immobilization, the NPs show characteristic AQ-COOH bands, indicating efficient PC incorporation into SNPs-NH_2. A small red-shift was observed in the maximum absorption band after immobilization of AQ-COOH, from 426 nm for AQ-COOH to 457 nm for SNPs-AQ. Additionally, the UV-visible spectra for an ethanolic solution of AQ-COOH and an ethanolic suspension of SNPs-AQ were recorded (Figure SI5). The spectrum of AQ-COOH exhibits two absorption maxima at 255 nm and 326 nm. In the case of SNPs-AQ, the UV-visible spectra were recorded before and after baseline correction due to light scattering associated with nanoparticles, observing a maximum at 255 nm. Both spectra of AQ-COOH and SNPs-AQ showed the same peak at 255 nm, indicating that the anthraquinone photocatalyst, once immobilized on SNPs, did not change its absorptions maxima. The absorbance at the maximum was compared to a calibration curve of homogeneous AQ-COOH (see Figs. SI5 and SI6), giving an AQ-COOH loading of 0.112 mmol per gram of nanomaterial. This value is comparable to that obtained by TGA analysis.

Taking into account that the photochemical and photophysical properties of substituted anthraquinones significantly depend on the electronic properties of the substituents, it was of interest to evaluate the fluorescence of PC before and after immobilization. Figure 2g shows the solid-state fluorescence emission spectra after exciting at 450 nm for SNPs-AQ, AQ-COOH and for a physical mixture of SNPs-NH_2 and AQ-COOH (3.9 wt %). As expected, SNPs-NH_2 precursor shows no signal in the study range. AQ-COOH presented an emission band with a maximum at 627 nm. After immobilization into de SNPs, the emission band of PC shifted to 604 nm. On the other hand, the maximum of the emission band for the physical mixture AQ-COOH and SNPs-NH_2 (626 nm) was similar to the AQ-COOH. The differences in band position between SNPs-AQ and AQ-COOH are related to changes in the electronic properties and chemical environment of the chromophore group. When the amide bond is formed and PC interacts with the surface of the SNPs, it is expected that the maximum emission would be modified.

The Infrared spectra (FT-IR) of AQ-COOH, SNPs-AQ, and SNPs-NH_2 were obtained (Figure SI4e-f). The spectra of SNPs-AQ and SNPs-NH_2 exhibited typical absorption bands for silica nanoparticles: a broad peak around 1098 cm^{-1} attributed to the stretching of Si-O-Si bonds; a peak at 468 cm^{-1} corresponding to the angular deformation of Si-O-Si groups; a broad band at 3419 cm^{-1} attributed to the stretching of O-H bonds of SiO-H groups,[26] and a shoulder at 947 cm^{-1} corresponding to the Si-OH vibration (in agreement to physis-absorbed surface water).[42] The FT-IR spectrum of AQ-COOH presented bands corresponding to the C=O bond stretching of carboxylic group and anthraquinone at 1701 and 1676 cm^{-1}, respectively, with OH deformation bending from the carboxylic group at 1435 cm^{-1}, and a peak at 702 cm^{-1} corresponding to the out-of-plane bending of Csp^2-H of aromatic anthraquinone ring.[43] In comparison, the spectrum of SNPs-AQ showed a small peak at 1678 cm^{-1} corresponding to the stretching of C=O bond of an amide group (amide I) together with a peak at 1594 cm^{-1} (amide II), indicating the formation of an amide bond with the anthraquinone PC. Furthermore, in the spectrum of SNPs-AQ a peak at 704 cm^{-1} corresponding to the out-of-plane bending of Csp^2-H of aromatic anthraquinone ring was observed, and the band related to the O-H vibration in carboxylic group at 1435 cm^{-1} of AQ-COOH disappeared.[44]

10.1002/chem.202303382

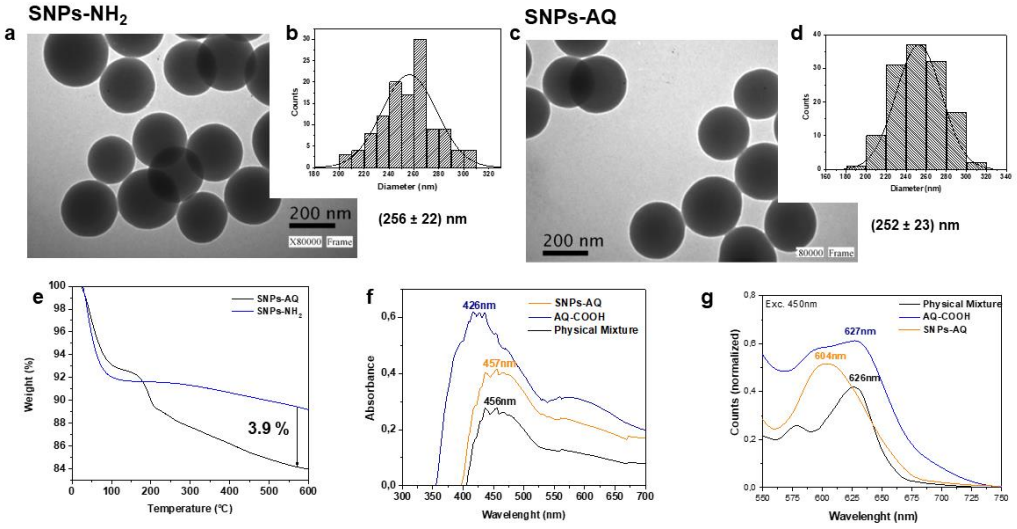

Figure 2. a) TEM micrograph and b) size distribution analysis for SNPs-NH_2. c) TEM micrograph and d) size distribution analysis for SNPs-AQ. e) Comparative TGA analysis for SNPs-NH_2 and SNPs-AQ. f) UV–vis diffuse reflectance (DR) from the solid state for SNPs-AQ, AQ-COOH, and the physical mixture of AQ-COOH + SNPs-NH_2. g) Comparative solid-state fluorescence spectroscopy for AQ-COOH, SNPs-AQ, and the physical mixture of AQ-COOH + SNPs-NH_2.

The effective incorporation of the AQ onto the SNPs materials was also supported by solid-state NMR spectroscopy and XPS. Figures SI7 shows the ^{1}H NMR spectra of SNPs-NH_2 and SNPs-AQ. The ^{1}H NMR spectra of SNPs-AQ presents a new band at ~6.5 ppm ascribed to the aromatic protons, which confirms the presence of the AQ PC. This band is absent in SNPs-NH_2 spectrum. On the other hand, XPS data confirmed the major contribution of SiO_2 and the relative atomic ratio of N atoms around 3% in the SNPs-NH_2 (Table SI2 and Figure SI8). The carbon content determined was higher in the SNPs-AQ material (C = 32 at%), doubling that of SNPs-NH_2 (C = 12 at%), while the percentage of N was similar in both samples (N = 3 at%). The higher contribution of the C 1*s* signals on SNPs-AQ are indicative of the successful grafting of AQ.[45]

Colloidal suspensions of SNPs-AQ in organic solvents with different polarities (ethanol (EtOH), isopropanol (2-PrOH), acetonitrile (MeCN) and acetone) were analyzed by Dynamic Light Scattering (DLS) techniques (Figure SI9), to control the stability and dispersion of this nanomaterial in different media. According to the DLS experiments (Table SI3), 2-PrOH was an appropriate solvent to disperse the SNPs-AQ nanoparticles.

Evaluation of photocatalytic activity

The catalytic activity of the heterogeneous photocatalyst SNPs-AQ was evaluated in the oxidative hydroxylation of arylboronic acid as a model reaction. Accordingly, the optimization of the reaction conditions was first performed employing the homogeneous catalysts AQ-COOH (10 mol%), phenylboronic acid (**1a**) as a substrate, under O_2 atmosphere in 2-propanol (2-PrOH) as a solvent, irradiated in a photoreactor equipped with two 400 W lamps. Table 1 summarized the results. Under this reaction condition, 65 % yield of phenol (**2a**) was quantified by GC analysis (entry 1, Table 1). The irradiation with a 3 W LED lamp (blue or white LED) decreased the yield of phenol **2a** (entries 2-3, Table 1). This issue can be related to the low molar extinction coefficient of AQ-COOH at 330 nm (Figure SI5), hence, light sources with high irradiance were required.

When the reaction was performed under dark conditions or without PC, phenol **2a** was detected in a very small amount in the reaction mixture (< 5 %, entries 4-5, Table 1). A marked decrease in reactivity was also observed by changing O_2 atmosphere by air (entry 6). These results indicated that the presence of AQ-COOH as PC, light, and O_2 are central to generate product **2a**, as previously found in recent reports.[17],[46]

When 3.5 mol% of PC was used, 76 % of yield of **2a** was obtained (entry 7, Table 1). However, for higher catalyst loading of AQ-COOH (5-10%), the yield of **2a** ranged between 62-65%, even after 10 h of irradiation (not tabulated). Thus, a smaller amount of AQ-COOH improves the yield of phenol **2a**. The drop of phenol **2a** yield observed by the increase of PC concentration, is probably due to the aggregation of the PC, decreasing their catalytic activity.[47]

Next, the solvent effect was evaluated exploring MeOH, EtOH, ^{t}BuOH, MeCN, and acetone (entries 8-12, Table 1). The reaction proceeded efficiently in solvents containing H atom at the C of carbinol group, such us 2-PrOH, EtOH and MeOH. By contrast, in solvents like acetone, MeCN, or ^{t}BuOH, the reaction was completely inhibited.

Others anthraquinone and xanthene derivatives (1,8-dihydroxianthraquinone, 1,5-diamineanthraquinone, and Eosin Y) were also explored as PCs under these mild homogeneous reaction conditions (entries 13-15, Table 1). These dyes did not produce **2a** under the evaluated conditions. Note that Paul and col.[38] described that phenol **2a** can be produced by the photoactivation of $PhI(OAc)_2$ by Eosin Y, in acetonitrile as a solvent and K_2CO_3 as a base. However, we explored this reaction, and phenol **2a** was produced with a 72 % of yield in the presence of $PhI(OAc)_2$ as an oxidant and K_2CO_3, without adding Eosin Y as PC in dark condition (see Table SI4 in the supporting information).

10.1002/chem.202303382

Table 1. Optimization reaction conditions for the oxidative hydroxylation of phenylboronic acid with homogeneous anthraquinones PC.[a]

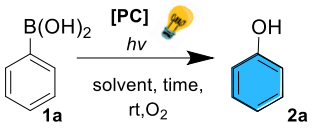

Entry	REACTION CONDITIONS: PC	Catalyst loading (mol %)	Time (h)	Solvent	Yield **2a** (%)[g]
1		10	5	2-PrOH	65
2[b]		10	24	2-PrOH	12
3[c]		10	24	2-PrOH	9
4[d]		10	5	2-PrOH	--
5[e]		--	5	2-PrOH	--
6[f]	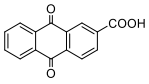 AQ-COOH	10	5	2-PrOH	5
7		**3.5**	**5**	**2-PrOH**	**76**
8		3.5	5	MeOH	30
9		3.5	5	EtOH	56
10		3.5	5	^{t}BuOH	--
11		3.5	5	Acetone	3
12		3.5	5	MeCN	--
13	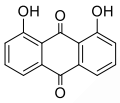 AQ-OH	10	5	2-PrOH	--
14	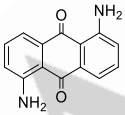 AQ-NH$_2$	10	5	2-PrOH	--
15	Eosin Y	10	5	2-PrOH	3

[a] Reaction conditions: 0.3 mmol substrate **1a**, the proper amount of PC, 5 mL of solvent, and O_2 atmosphere, were irradiated for the time indicated, employing two 400 W lamps. [b] Under blue LED irradiation. [c] Under white LED irradiation. [d] Without light (dark condition). [e] Without PC. [f] Under air atmosphere. [g] Yield of **2a** quantified by GC analysis.

Following, the catalytic activity of the heterogeneous photocatalyst SNPs-AQ was explored in the optimized reaction conditions (Table 2). The photostimulated reaction (λ > 350 nm, two 400 W lamps) was performed with 0.22 mmol of substrate **1a** and 50 mg of SNPs-AQ which contains 0.0077 mmol of AQ-COOH, representing 3.5 mol % of PC relative to phenylboronic acid. Under this condition, 74 % yield of phenol **2a** was obtained (entry 1, Table 2). Thus, the immobilized anthraquinone AQ-COOH maintained its catalytic activity. Moreover, the heterogeneous PC produced similar results to those of homogeneous AQ-COOH, under the same reaction conditions (entry 7, Table 1). Likewise, reactions performed with 3 W LED lamps (blue and white) did not provide good yields of phenol **2a** (entries 2-3, Table 2). With a smaller amount of catalyst (25 mg, 1.75 mol%), the yield of **2a** decreased to 53 % after 7.5 h of irradiation (entry 4, Table 2). When the catalyst loading was increased at almost 5.25 mol %, 74 % of yield of **2a** was achieved after 5 h (entry 5, Table 2). However, a slurry reaction mixture was obtained, which was difficult to stir and irradiate. Furthermore, product **2a** was not observed in the reactions carried out under dark conditions or in the presence of the functionalized nanoparticles SNPs-NH_2 (entries 6-7, Table 2). These results confirm not only that AQ-COOH is the catalytically active species, but also that the silica support does not contribute to product formation. Thus, the SNPs mainly act as an inert support, enabling the subsequent separation, recovery, and reuse of the PC.

Table 2. Oxidative hydroxylation of phenylboronic acid (**1a**) in the presence of heterogeneous SNPs-AQ.[a]

Entry	REACTION CONDITIONS: PC (mol %)	Time (h) Solvent	Yield **2a** [%f]
1	50 mg SNPs-AQ (3.5 mol % AQ)	5	74
2[b]	50 mg SNPs-AQ (3.5 mol % AQ)	24	12
3[c]	50 mg SNPs-AQ (3.5 mol % AQ)	24	9
4	25 mg SNPs-AQ (1.75 mol % AQ)	7.5	53
5	75 mg SNPs-AQ (5.25 mol % AQ)	5	74
6[d]	50 mg SNPs-AQ (3.5 mol % AQ)	5	--
7[e]	50 mg SNPs-NH_2 (0 mol % AQ)	5	--

[a] Reaction conditions: 0.22 mmol substrate **1a**, catalyst (catalyst loading expressed in mol% with respect to **1a**), 5 mL of 2-PrOH, and O_2 atmosphere, were irradiated for the indicated time, employing two 400 W lamps. [b] Under blue LED irradiation. [c] Under white LED irradiation. [d] Without light (dark condition). [e] Without PC. [f] Yield of **2a** quantified by GC analysis.

In addition, the substrate scope was explored by carrying out a series of reactions with substituted arylboronic acids with the heterogeneous photocatalyst SNPs-AQ (Table 3). In all cases, the reactions were performed in the previously optimized reaction conditions with 50 mg of SNPs-AQ under irradiation for 5 h, in the presence of O_2 and 2-PrOH as solvent.

10.1002/chem.202303382

Table 3. Substrate scope evaluation in the oxidative hydroxylation of arylboronic acids in the presence of heterogeneous photocatalyst SNPs-AQ. [a,b]

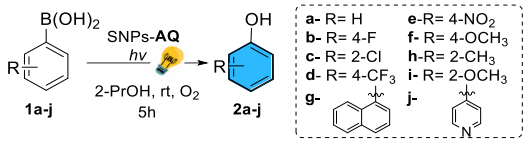

Substrate	Product	Substrate	Product
 **1a**	 **2a**: 74%	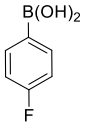 **1b**	 **2b**: 100%
 **1c**	 **2c**: 24% **2c**: 50% (8h)	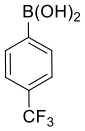 **1d**	 **2d**: 59%
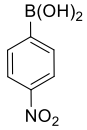 **1e**	 **2e**: 65%	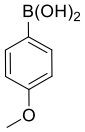 **1f**	 **2f**: 57%
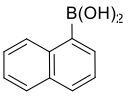 **1g**	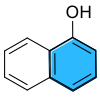 **2g**: 100%	 **1h**	 **2h:** 86%
 **1i**	 **2i**: 31% (8h)	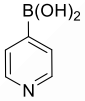 **1j**	 **2j**: 47% (8h)

[a] Reaction conditions: 0.22 mmol substrate, 50 mg SNPs-AQ (3.5 mol % with respect to **1a-j**), 5 mL of 2-PrOH, O_2 atmosphere, were irradiated for the indicated time using two 400 W lamps. [b] Yield of **2a-2j** quantified by GC analysis.

Phenols were obtained in good yields with both electron-withdrawing and electron-donating functional groups (**2b-2j**, Table 3). These results show that SNPs-AQ efficiently catalyzes the oxidation of arylboronic acids, even with sterically hindered substrates, such as 2-chlorophenylboronic acid **1c**, 2-naphthaleneboronic acid **1g**, and 2-methylphenylboronic acid **1h**. However, lower yield was obtained with 2-methoxyphenylboronic acid **1i**, even after 8 h of irradiation. In some cases, it was necessary to adjust the reaction time according to the substrate, for example with 2-chlorophenylboronic acid (**1c**) and the heterocyclic 4-pyridinyl-boronic acid (**1j**), which provide the corresponding products **2c** and **2j,** obtained in 50% and 47 % yields, respectively.

In order to gain insight into the heterogeneous nature of the SNPs-AQ catalyst, a filtration test under the optimized reaction conditions was conducted (Figure 3). In this test, the reaction mixture was centrifuged to remove the heterogeneous PC after 2.5 h of irradiation; and the obtained liquid phase was allowed to react under irradiation for additional 2.5 h in the presence of O_2. A control experiment was also performed to monitor the progress of the reaction over time. The reaction was almost inhibited after the filtration process (Figure 3). This result suggests that the active catalytic species was mainly removed by centrifugation and filtration, supporting that SNPs-AQ catalyst followed a heterogeneous pathway. The negligible amount of AQ-COOH released from SNPs during the reaction progress could be responsible for the small amount of phenol **2a** produced after the filtration (< 10 %).

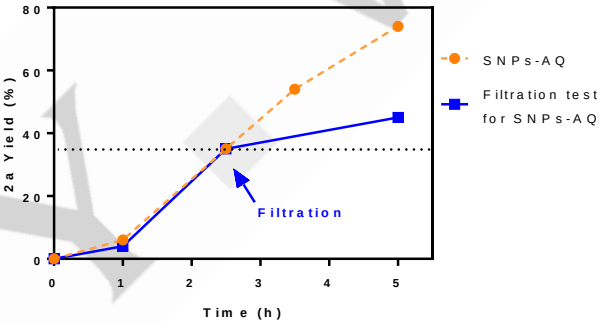

Figure 3. Comparison of the progress of the reaction under standard conditions (orange dash lines and circle) and after performing the filtration test (blue line and squares).

Based on the results described above, as well as those previously reported,[46],[48] the mechanism proposed for the oxidative hydroxylation of arylboronic acids is that depicted in Figure 4. At first, the heterogeneous SNPs-AQ PC is excited under visible-light irradiation to generate SNPs-AQ*, which abstracts a hydrogen atom from 2-PrOH to produce 2-isopropanol radical (**3**) and reduced SNPs-AQH • .[49] The radical **3** traps molecular oxygen affording the peroxy radical **4**. The intermediate **4** abstracts H atom from the SNPs-AQH • species, regenerating the SNPs-AQ PC and producing the hydroxyl hydroperoxide **5**. The hydroxy hydroperoxide **5** fragments to acetone and hydrogen peroxide. Combining hydrogen peroxide with the arylboronic acid results in the species boron peroxo **6**.[50],[51],[52],[53] Finally, the formation of the phenol (**2a**) takes place by the rearrangement of **6** into **7** followed by its hydrolysis.

10.1002/chem.202303382

RESEARCH ARTICLE

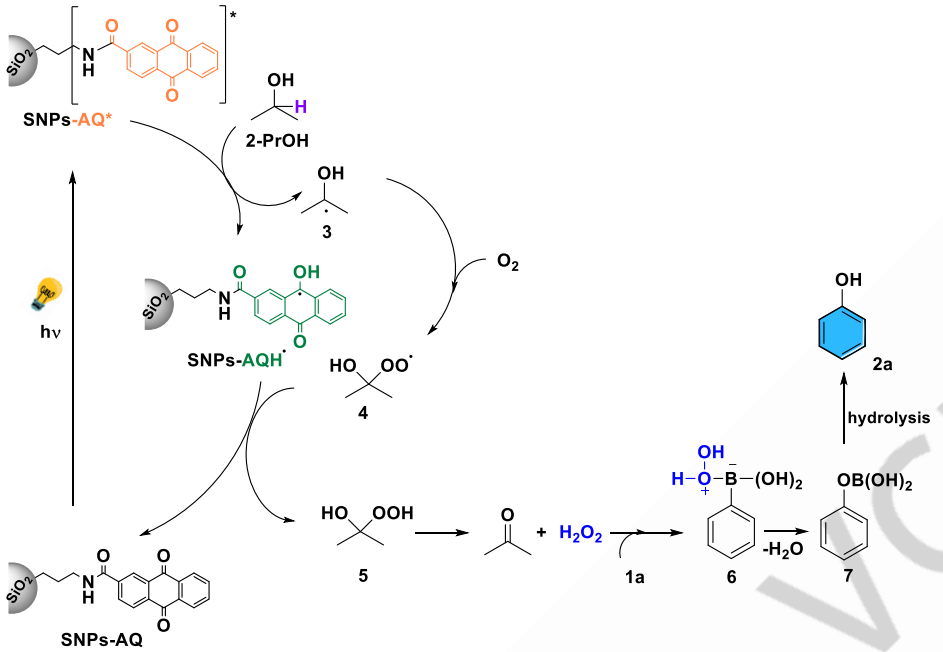

Figure 4. Proposed mechanism for the oxidative hydroxylation of phenylboronic acid (**1a**) to obtain phenol (**2a**) in the presence of SNPs-AQ heterogeneous catalyst.

It should be noted that, the mechanism relies on the presence of hydrogen bonded to the carbinol carbon for the formation of radical SNPs-AQH •. Consequently, when the reaction is carried out in solvents lacking this type of hydrogen, such as ^{t}BuOH, acetone and MeCN (Table 1, entries 10-12), the reaction does not occur. However, in solvents like MeOH and 2-PrOH, where the required hydrogen is present, the reaction takes place (Table 1, entries 7 and 8). The slower reaction rate observed in MeOH compared to 2-PrOH can be attributed to the formation of a less stable primary radical, in contrast to the more stable tertiary radical formed when the reaction is carried out in 2-PrOH. Furthermore, DLS analysis showed that the SNPs-AQ were less aggregated in 2-PrOH, which favored a greater availability of PC for the reaction.

To demonstrate the formation of H_2O_2 in the reaction medium, we performed a control experiment in which the PC (SNPs-AQ) and 2-PrOH were irradiated in the presence of O_2 for 5 h. Then, we perform the detection of H_2O_2 by reaction with KI/AcOH, observing the formation of the blue [starch-I_2] complex (see Supporting Information, section 6).

Likewise, the generation of H_2O_2 as reagent was explored in a control organic transformation to obtain epoxide products (Figure 5a). In a similar fashion, first H_2O_2 was generated by irradiation of a mixture SNPs-AQ (or AQ-COOH) and 2-PrOH. Then under dark reaction conditions, the atmosphere was changed to N_2, and *E*-chalcone (**8**) and 0.8 eq of KOH were added to the mixture (Figure 5b). The reaction was stirred for 1 h. Finally, the product distribution was analyzed by ^{1}H NMR. In the presence of both homogeneous and heterogeneous PCs, epoxide **9** was observed in good yields. In consequence, we can assume that H_2O_2 is the key intermediate formed by anthraquinone PC under the evaluated reaction conditions. It is important to highlight that, heterogeneous SNPs-AQ produced 94 % yield of epoxide **9**, while homogeneous AQ-COOH gave only 60 % yield of **9**.

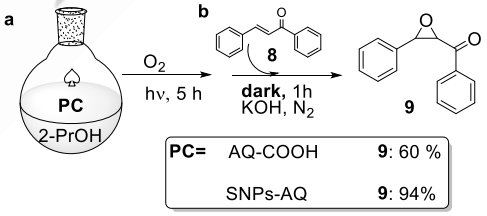

Figure 5. Control experiment for the epoxidation of *E*-chalcone by formation of H_2O_2.

Since reusability is a key feature of any heterogeneous catalyst, as it provides information on catalytic stability with continuous catalytic runs, a recyclability test was performed (Figure 6). The experiments were carried out in the oxidative hydroxylation of 4-fluorphenylboronic acid (**1b**), employing the optimized reaction conditions and SNPs-AQ as catalysts. After each reaction cycle the catalyst was centrifuged, and the solid was washed with 2-PrOH. The SNPs-AQ was then dried, and reused in the next catalytic cycle. Under this protocol, five catalytic cycles of reuse were achieved (Figure 6).

10.1002/chem.202303382

RESEARCH ARTICLE

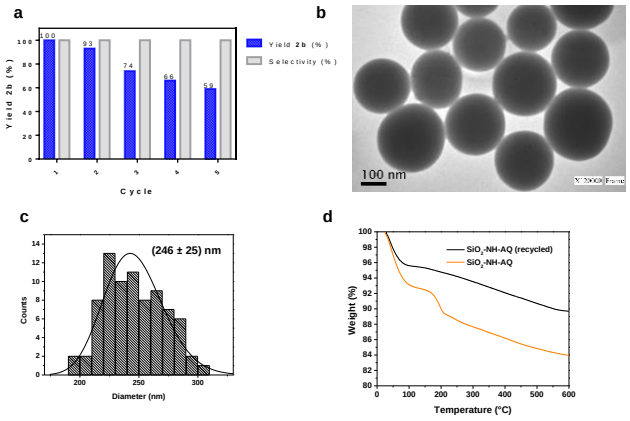

Figure 6. (a) Recycling experiment for SNPs-AQ employing 4-fluorphenylboronic acid (**1b**) as a substrate. (b) TEM analysis and (c) size analysis for SNPs-AQ catalyst after 5 catalytic cycles. (d) Comparative TGA analysis for SNPs-AQ before and after recycling.

Additionally, a physical mixture using 100 mg of SNPs-NH_2 and 3.9 mg of AQ-COOH (with no covalent bonding of PC to SNPs-NH_2) was prepared, and evaluated as catalyst in the reaction of **1b** in 2-PrOH. After 5 hours of irradiation the complete formation of **2b** was achieved. Subsequently, the reuse of this physical mixture was evaluated after centrifugation and washing of the solid with 2-PrOH. After the second cycle of irradiation, only a 5% yield of **2b** was detected, demonstrating that all the AQ-COOH had been removed from this physical mixture (which is completely soluble in 2-PrOH at this concentration). This result supports the covalent bonding between AQ-COOH and SNPs-NH_2 in SNPs-AQ.

Although SNPs-AQ proved to be a recyclable catalyst, the catalytic activity progressively decreased reaching 59 % yield of **2b** after the fifth catalytic cycle. TEM analysis of the heterogeneous photocatalyst after all recycle cycles showed that the SNPs-AQ nanocatalyst maintained its structure and morphology after the catalytic reaction, observing a slight decrease in the diameter of the particles (Figure 6b and 6c). The FT-IR spectrum of recycled SNPs-AQ photocatalyst (Figure SI12) exhibited the bands corresponding to the stretching of C=O bond of the anthraquinone PC at 1678 cm^{-1} and out-of-plane bending of Csp^2-H of aromatic anthraquinone ring at 704 cm^{-1}. Finally, through TGA (Figure 6d), a slight loss of organic matter can be observed when comparing the spectra of SNPs-AQ before and after recycling. Similarly, the UV-vis absorption spectrum of SNPs-AQ before and after recycling exhibits an absorption band at the same position but with different intensity, indicating the loss of AQ-COOH (See Figure S13 in Supporting Information). Therefore, the lower reaction yield obtained after the fifth cycle may be attributed to the slight loss of PC.

Catalyst deterioration could be produced by parameters such as solvent and chemical environment in the reaction mixture. Prolonged periods of irradiation (5 h per reaction) could also lead to deactivation of photocatalyst.[54] Nevertheless, the catalytic activity in the final cycle was considerably high taking into account that the PC was active for 25 h of irradiation, with an accumulative turnover number (TON) of 112, demonstrating the potential advantage of preparing heterogeneous PC.

The comparison of the catalytic activity of SNPs-AQ with other heterogeneous PCs in the oxidative hydroxylation of arylboronic acid is shown in Table 4. SNPs-AQ demonstrated promising features as a PC, exhibiting a higher turnover frequency value (TOF= 3.7 h-1) than other heterogeneous PCs prepared by the immobilization of AQ-COOH. On the other hand, heterogeneous PCs prepared by the combination of Ru or Ir complexes with inorganic metal oxides displayed higher catalytic activity than SNPs-AQ in phenol production (Table 4),[54,55] even though the elevated cost of organometallic complexes reduces their widespread utilization. Recently, carbon-based heterogeneous nanomaterials were successfully explored as PCs in the hydroxylation of arylboronic acid.[56,57] However, the challenging preparation of these materials makes their application

Table 4. Comparison of the catalytic activity of SNPs-AQ with heterogeneous PC in the oxidative hydroxylation of phenylboronic acid.

Catalytic system	PC (catalyst load)	Support	Reaction conditions	Time (h)	Yield of **2a** (%)	TOF (h^{-1})	Citation
AQ-PHEMA	AQ-COOH (3 mol %)	PHEMA polymer	Air, Dioxane, DIPEA (2 equiv), Purple LED lamp	27	99	1.2	[17]
GW-AQ	AQ-COOH (25 mg)	Glass wool	O_2, MeCN:H_2O, DIPEA (5 equiv), Blue LED lamp	6	3	--	[25]
SNPS-AQ	AQ-COOH (3.5 mol %)	SNPs	O_2, 2-PrOH, White lamp	5	64	3.7	This work
Ru-SiO_2	$[Ru(bpy)_3]^{2+}$ (0.5 mol%)	Mesoporous silica	O_2, DMF, White lamp	3	96	6.4	[55]
Ir-Al_2O_3	[Ir-(dcabpy)$(ppy)_2$] (0.1 mol%)	Al_2O_3	Air, DMF, DIPEA (2 equiv), Blue LED lamp	84	91[a]	11	[54]
C_{70}	C_{70} fullerene (0.05 mol%)	--	O_2, $CHCl_3$, DIPEA (2 equiv), Blue LED lamp	12	99	165	[56]
DBOV-COF	dibenzo[*hi,st*]ovalene (3 mg)	--	Air, MeCN, TEA (1.5 equiv), White LED lamp	5	97	58	[57]

[a] 4-methoxyphenylboronic acid (**1f**) was employed as substrate

currently impractical. Furthermore, in the present methodology, the use of a sacrificial donor was avoided, which is an important aspect, since the SNPs-AQ catalyst allowed to obtain phenols in good yields without employing large amounts of amine derivatives like DIPEA or triethylamine, which are toxic reagents. Moreover, in comparison with others heterogeneous PC shown in Table 4, our reaction protocol employs a solvent recommended by the CHEM21 selection guide (2-PrOH),[58] excluding the use of problematic or hazardous solvents, such as DMF or $CHCl_3$.[55,56] Thus, the developed catalytic system improves the use of AQ-COOH as PC and contributes to the design of eco-friendly reaction conditions for organic transformations.

By a simple strategy, we were able to improve the catalytic activity and recyclability of an anthraquinone photocatalyst, and design mild and environmental benign reaction conditions for the oxidative hydroxylation of arylboronic acid. The silica nanoparticle support exhibited great properties for their use as a support for PCs, since the structure and morphology of SNPs were not changed after immobilization of AQ-COOH and after catalytic reactions take place. These results indicate that SNPs-AQ is a highly versatile catalyst for the oxidative conversion of arylboronic acids into phenols.

Conclusion

In conclusion, the heterogeneous photoredox nanocatalyst SNPs-AQ was prepared by a simple and straightforward methodology. The developed strategy enabled the synthesis of SNPs-AQ under sustainable reaction conditions, incorporating approximately 3.9 wt% of the organic dye (AQ-COOH) into spherical SiO_2 NPs. This process resulted in minimal alteration of the SNPs structure while retaining the activity of the organic dye.

The SNPs-AQ efficiently catalyzed the oxidative hydroxylation of arylboronic acids to phenols employing visible light, O_2 as an oxidant and 2-PrOH as a solvent. Immobilization over SNPs does not alter the catalytic activity of AQ-COOH since the heterogeneous system showed a catalytic activity similar to that of the corresponding homogeneous catalyst. Furthermore, it also improved the recovery and reuse of the PC, being SNPs-AQ recycled for at least five times. The experimental results indicate the formation of H_2O_2 as a key intermediate in the oxidative hydroxylation reaction, which could be employed in other important organic reactions, like epoxidation of alkenes.

Finally, the simple developed heterogeneous system showed promising catalytic activity to develop further organic reaction transformations under sustainable reaction conditions.

Experimental Section

Material and methods

All chemicals were reagent grade and were used as received from the manufacturer. Anthraquinone 2-carboxylic acid (Sigma Aldrich®), 1,8-dihydroxianthraquinone (Sigma Aldrich®), 1,5-diamineanthraquinone (Sigma Aldrich®), Eosin Y (Sigma Aldrich®), ammonium hydroxide (NH_4OH, 28 % w/w, Anhedra®), tetraethyl orthosilicate (TEOS, Sigma Aldrich®), (3-aminopropyl)-triethoxysilane (APTES, Sigma Aldrich®), *N,N´*-dicyclohexylcarbodiimide (DCC Sigma Aldrich®), 1-hydroxibenzotriazole (HOBt, Sigma Aldrich®), phenylboronic acid (Sigma Aldrich®), 4-fluorphenylboronic acid (Sigma Aldrich®), 2-chlorophenylboronic acid (Sigma Aldrich®), (4-trifluormethyl)phenylboronic acid (Sigma Aldrich®), 4-nitrophenylboronic acid (Sigma Aldrich®), 4-anisylboronic acid (Sigma Aldrich®), 2-tolylboronic acid (Sigma Aldrich®), 1-naphtylboronic acid (Sigma Aldrich®), 2-anisylboronic acid (Sigma Aldrich®), 4-pyridinyl-boronic acid (Sigma Aldrich®), KOH (Cicarelli®), K_2CO_3 (Anedra®), (Diacetoxyiodo)benzene ($PhI(OAc)_2$, Sigma Aldrich®); benzophenone (Sigma Aldrich®), *p*-nitroacetophenone (Sigma Aldrich®). Ethanol 98 % (EtOH, Porta®), 2-propanol (2-PrOH, Cicarelli®), methanol (MeOH, Cicarelli®), *t*-butanol (*t*-BuOH, Cicarelli®), acetonitrile (MeCN, J. T. Baker®); tetrahydrofurane (THF, Sintorgan®) and anhydrous Na_2SO_4 (Anhedra®) were used as received. Acetone and ethyl acetate solvents were analytical grade and distilled before use. Milli-Q-Millipore water was employed in all the experiments. Silica gel (0.063–0.200 mm) was used in column chromatography.

The SNPs were characterized by Transmission Electron Microscopy (TEM) using a JEM-Jeol 1120 microscope operating at 80 kV, available at the Research Institute IPAVE- INTA-CIAP in Córdoba, Argentina. SEM microscopy was performed in a SEM - Zeiss Sigma 360 (Lamarx-UNC). Thermogravimetric analyses (TGA) were performed in TA Instruments –Discovery TGA 55 (UNITEFA-CONICET-UNC). Solid state fluorescence and UV–vis diffuse reflectance were performed in Horiba Nanolog and UV–vis RD Stellar Net Black-Comet spectrophotometer; respectively. Characterization by XRD was performed using a PANalytical X'Pert Pro diffractometer (40 kV, 40 mA) in Bragg–Brentano reflection geometry with Cu Ka radiation (l = 1.5418 A). Data were gathered between 101 and 701 (2y) in steps of 0.02 and a counting time of 24 s. The refinement of the crystal structure was performed by the Rietveld method using the FULLPROF program. FT-IR spectra were collected on an infrared microscope (Nicolet iN10, Thermo Scientifics, USA). Samples contained in KBr discs were scanned from 4000 to 400 cm^{-1} and the recording conditions were: normal resolution, sample scan, 64 s^{-1}. The spectra were recorded, processed and analyzed using the EZ OMNIC ESP 8.3.103 program. DLS measurements were performed by using a Delsa Nano C instrument (Beckman Coulter, Osaka, Jp.). The hydrodynamic apparent diameter (d_H) was determined by Photon Correlation Spectroscopy at a controlled temperature of 25 °C in triplicate, using glass cuvettes. Intensity autocorrelation functions were analyzed with the Delsa Nano 2.20 software (Beckman Coulter, Osaka, Jp). Number-weighted particle size distribution was calculated assuming spherical morphology with constant refractive index.

A commercial Thermo Scientific K-Alpha X-ray photoelectron spectrometer (XPS) system (LAMARX, FaMAF-UNC), equipped with a hemispherical energy analyzer and a monochromated X-ray source was used for surveying the photoemission spectra. The base pressure measured in the main chamber was in the low 10^{-9} mbar range. The photoionization of

10.1002/chem.202303382

the samples was induced by monochromatized Al Kα photons at 1486 eV. All the spectra were adjusted to the main spurious C *1s* peak at 284.8 eV. To avoid any charging effects during measurement (typically observed in semiconductor-isolated systems), a flood gun to compensate the charge was used. The overcompensation effects by adjusting the spectra during measurement were also tested.

^{1}H *solid-state* Nuclear Magnetic Resonance (*ss*-NMR) experiments were acquired with a spectrometer equipped with a 14.1 T narrow bore magnet operating at a Larmor frequency of 600.09 MHz for ^{1}H. Powdered samples were packed into 2.5 mm ZrO_2 rotors and rotated at room temperature at magic angle spinning (MAS) rates of 30 kHz. For ^{1}H chemical shifts (expressed in ppm) are relative to TMS (δ^1H = 0 ppm).

Gas chromatographic analysis were performed on a gas chromatograph with a flame ionization detector, and equipped with the following columns: VF-5 30 m × 0.20 mm × 0.25 µm column. Gas Chromatographic/Mass Spectrometer analyses were carried out on a GC/MS QP 5050 spectrometer equipped with a VF-5ms, 30 m × 0.25 mm × 0.25 µm column. UV-vis determinations were performed using a SHIMATZU UV-Vis UV-1800 series. ^{1}H NMR were conducted on a High-Resolution Spectrometer Bruker Advance 400, in $CDCl_3$ as solvent.

Photoinduced reactions were conducted with blue LED (λ= (465 ± 20) nm) lights performing at 3W of potency and 700 mV of current emission spectra (Figure SI1) and HPIT 400W lamps (λ≥ 350 nm, Figure SI2).

Synthesis of SiO_2 nanoparticles functionalized with amino group (SNPs-NH_2)

In a 100 mL round bottom flask equipped with a magnetic stir bar, were placed 60 mL of ethanol and 4.8 mL of NH_4OH aqueous solution (28 % w/w). After vigorously stirring of the mixture for 5 min, 2.5 mL of TEOS were added. This mixture was stirred for 24 h at room temperature. Then, 200 µL of APTES were added, and the mixture was stirred for another 24 h. For purification of SNPs-NH_2, the reaction mixture was centrifuged for 8 min at 3500 rpm, the supernatant was discarded, and the white solid was washed with ethanol, sonicated by 5 min and centrifuged again. This procedure was repeated 3 times. Finally, the SNPs-NH_2 were dried under the air and at room temperature for 24 h. After this procedure, 670 mg of SNPs-NH_2 were recovered.

Immobilization of AQ-COOH into SNPs-NH_2

In a 10 mL Schlenk tube, equipped with a magnetic stir bar and under nitrogen atmosphere, 20 mg of anthraquinone 2-carboxylic acid, 62 mg of HOBT (5 eq.); 83 mg DCC (5 eq.) and 4 mL of acetone were placed. The reaction mixture was heated under reflux for 1 h. After being cooled to room temperature, 200 mg of SNPs-NH_2 were added under nitrogen atmosphere, and the mixture was allowed to react for 24 h. The as-obtained SNPs-AQ were centrifuged at 3500 rpm for 8 min, and then suspended in THF; sonicated for 5 min and centrifuged for 8 min. Then, SNPs-AQ were washed with acetone, MeCN and ethanol (3 times), following the same procedure. Finally, the SNPs-AQ were dried under the air and at room temperature for 24 h. After this procedure, 175 mg of pale-yellow SNPs-AQ were recovered.

Representative procedure for the oxidative hydroxylation of phenylboronic acid reaction catalyzed by homogeneous AQ-COOH photocatalyst

In a 5 mL scintillation vial equipped with a magnetic stir, 37.6 mg of phenylboronic acid (0.30 mmol), 7.6 mg of AQ-COOH (0.03 mmol) and 5 mL of 2-PrOH were placed. The vial was sealed with a Teflon plug and O_2 passed through for 5 min to saturate the solution. Next, the vial was placed into the photochemical reactor, and was irradiated under vigorous magnetic stirring for 5 h with an O_2 balloon. After this time, 1 mL of benzophenone solution (10 mg/mL) in ethyl acetate was added to the reaction mixture and a sample was analyzed by GC, and the products were compared with pure sample of phenol. The phenol product was quantified by GC employing benzophenone as internal standard.

Representative procedure for the oxidative hydroxylation of arylboronic acid reaction catalyzed by heterogeneous SNPs-AQ photocatalyst

In a 5 mL scintillation vial equipped with a magnetic stir, were placed 0.22 mmol of arylboronic acid, 50 mg of SNPs-AQ (0.0077 mmol of AQ-COOH) and 5 mL of 2-PrOH. The vial was sealed with a Teflon plug and O_2 passed through for 5 min to saturate the solution. Next, the vial was placed into the photochemical reactor, and was irradiated under vigorous magnetic stirring for 5 h with an O_2 balloon. After this time, 1 mL of benzophenone solution (10 mg/mL) was added to the reaction mixture. Then, the mixture was centrifuged at 3500 rpm for 8 min and the supernatant was analyzed by GC employing benzophenone as internal standard.

Representative procedure for the epoxidation of alkenes

A dry 2-propanol solution (3 mL) of AQ-COOH (1.5 mg, 0.006 mmol) in a 5 mL scintillation vial equipped with a magnetic stir vial was sealed with a Teflon plug and O_2 passed through for 5 min to saturate the solution. Next, the vial was placed into the photochemical reactor, and was irradiated under vigorous magnetic stirring for 5 h with an O_2 balloon. Then, (*E*)-chalcone (62.5 mg, 0.3 mmol) and KOH aq (1 M, 240 µL, 0.24 mmol) were added to the mixture, followed by 1 h of stirring under the N_2 atmosphere. The product was extracted with Et_2O, dried with Na_2SO_4, and then, the solvent was removed under reduced pressure. The crude reaction was analyzed by ^{1}H NMR spectroscopy employing *p*-nitroacetophenone as internal standard.

Filtration test

In a 5 mL scintillation, 26.9 mg of phenylboronic acid, 5 mL of 2-PrOH and 50 mg of SNPs-AQ were added. The vial was sealed with a septum and a Teflon membrane, and placed under O_2 atmosphere. The reaction was irradiated for 2.5 h with an O_2 balloon. After this time, the mixture was centrifuged, separating the precipitate from the supernatant. The supernatant was taken, placed in a clean vial, reloaded with O_2 and irradiated for 2.5 h. After the reaction time, the mixture was processed in the same way as the reaction with the heterogeneous catalyst to determine the product yield and conversion.

Recyclability Test

In a 5 mL scintillation vial, 12.5 mg of 4-fluorphenylboronic acid, 20 mg of SNPs-AQ and 2.5 mL 2-PrOH were placed, which was sealed with a septum and a Teflon membrane, and connected to a balloon with O_2, to irradiate the mixture for 5 h. Then, the mixture was centrifuged, the precipitate was separated from the supernatant by centrifugation at 8000 rpm for 5 minutes. The supernatant was quantified by GC to determine product formation, and the recovered SNPs-AQ was air-dried for use again in another reaction. This procedure was repeated for five times.

Supporting Information

The authors have cited additional references within the Supporting Information. [59-61] General experimental methods and equipment, materials, characterization data, spectroscopic studies and Figures SI1-SI11 and Tables SI1-SI4 (PDF).

Acknowledgements

This work was supported by CONICET (PUE: 22920160100013CO and PIP No 0100271), Agencia Nacional de Promoción Científica y Tecnológica, ANCyT (PICT 2018-3943, PICT 2019-2184, PICT 2021-Cat-I-136, PICT 2021-GRFTI-376) and Secretaría de Ciencia y Tecnología, Universidad Nacional de Córdoba (SECyT). M. G. M. gratefully acknowledge receipt of fellowship from CONICET. The authors acknowledge the use of a fluorometer acquired with SeCyT-UNC funds through PRIMAR-TP: 32520170100204CB01 and Agustín Green by the technical support. The authors would like to express their gratitude to Professor Veronica Brunetti (INFIQC) and Professor Maximiliano Burgos (INFIQC) for their valuable assistance with XPS measurements and FT-IR analysis, respectively.

Keywords: Heterogeneous Photocatalyst • Anthraquinone • Aerobic Hydroxylation • Hydrogen Atom Transfer • Catalysis

References

[1] N. Corrigan, S. Shanmugam, J. Xu, C. Boyer, *Chem. Soc. Rev.* **2016**, *45*, 6165–6212.
[2] M. H. Shaw, J. Twilton, D. W. C. MacMillan, *J. Org. Chem.* **2016**, *81*, 6898–6926.
[3] N. A. Romero, D. A. Nicewicz, *Chem. Rev.* **2016**, *116*, 10075–10166.
[4] C. K. Prier, D. A. Rankic, D. W. C. MacMillan, *Chem. Rev.* **2013**, *113*, 5322–5363.
[5] J. Cervantes-González, D. A. Vosburg, S. E. Mora-Rodriguez, M. A. Vázquez, L. G. Zepeda, C. Villegas Gómez, S. Lagunas-Rivera, *ChemCatChem* **2020**, *12*, 3811–3827.
[6] S. Lerch, L. N. Unkel, P. Wienefeld, M. Brasholz, *Synlett* **2014**, *25*, 2673–2680.
[7] M. Brasholz, *Science of Synthesis: Photocatalysis in Organic Synthesis*, Thieme, Stuttgart, **2018**.
[8] S. Gisbertz, B. Pieber, *ChemPhotoChem* **2020**, *4*, 456–475.
[9] R. Y. Liu, S. Guo, S.-X. L. Luo, T. M. Swager, *Nat. Commun.* **2022**, *13*, 2775–2783.
[10] I. Ghosh, J. Khamrai, A. Savateev, N. Shlapakov, M. Antonietti, B. König, *Science* **2019**, *365*, 360–366.
[11] L. Zeng, X. Guo, C. He, C. Duan, *ACS Catal.* **2016**, *6*, 7935–7947.
[12] C. H. Mak, X. Han, M. Du, J.-J. Kai, K. F. Tsang, G. Jia, K.-C. Cheng, H.-H. Shen, H.-Y. Hsu, *J. Mater. Chem. A* **2021**, *9*, 4454–4504.
[13] C.-A. Wang, Y.-W. Li, X.-L. Cheng, J.-P. Zhang, Y.-F. Han, *RSC Adv.* **2017**, *7*, 408–414.
[14] S. Füldner, R. Mild, H. I. Siegmund, J. A. Schroeder, M. Gruber, B. König, *Green Chem.* **2010**, *12*, 400–406.
[15] G. Kumar, P. Solanki, M. Nazish, S. Neogi, R. I. Kureshy, N. H. Khan, *J. Catal.* **2019**, *371*, 298–304.
[16] A. Savateev, M. Antonietti, *ACS Catal.* **2018**, *8*, 9790–9808.
[17] Y. Chen, J. Hu, A. Ding, *RSC Adv.* **2020**, *10*, 7927–7932.
[18] F. Wang, D. Yu, Y. Chen, J. Sun, J. Wang, M. Zhou, *Chem. Asian J.* **2021**, *16*, 4087–4094.
[19] L. Zhao, W. Cai, G. Ji, J. Wei, Z. Du, C. He, C. Duan, *Inorg. Chem.* **2022**, *61*, 9493–9503.
[20] R. M. Abdelhameed, M. Abu-Elghait, M. El-Shahat, *J. Photochem. Photobiol. A* **2022**, *423*, 113572.
[21] H. Kim, Y. Choi, S. Hu, W. Choi, J.-H. Kim, *Applied Catalysis B: Environmental* **2018**, *229*, 121–129.
[22] P. Trigueiro, F. A. R. Pereira, D. Guillermin, B. Rigaud, S. Balme, J.-M. Janot, I. M. G. Dos Santos, M. G. Fonseca, P. Walter, M. Jaber, *Dyes and Pigments* **2018**, *159*, 384–394.
[23] S. M. Soria-Castro, B. Lebeau, M. Cormier, T. Neunlist, T. J. Daou, J.-P. Goddard, *Eur. J. Org. Chem.* **2020**, *2020*, 1572–1578.
[24] I. Rosa-Pardo, M. Roig-Pons, A. A. Heredia, J. V. Usagre, A. Ribera, R. E. Galian, J. Pérez-Prieto, *Nanoscale* **2017**, *9*, 10388–10396.
[25] R. I. Teixeira, N. C. de Lucas, S. J. Garden, A. E. Lanterna, J. C. Scaiano, *Catal. Sci. Technol.* **2020**, *10*, 1273–1280.
[26] R. C. De Souza Oliveira, R. J. Corrêa, R. S. P. Teixeira, D. D. Queiroz, R. Da Silva Souza, S. J. Garden, N. C. De Lucas, M. D. Pereira, J. S. Bello Forero, E. C. Romani, E. S. Ribeiro, *J. Photochem. Photobiol. B* **2016**, *165*, 1–9.
[27] J. Flores, P. Moya, F. Bosca, M. L. Marin, *Catal. Today* **2023**, *413–415*, 113994.
[28] N. Mahmound, J. Awassa, J. Toufaily, B. Lebeau, T. J. Daou, M. Cormier, J.-P. Goddard, *Molecules* **2023**, *28*, 549–564.
[29] S. E. Mora-Rodríguez, A. Camacho-Ramírez, J. Cervantes-González, M. A. Vázquez, J. A. Cervantes-Jauregui, A. Feliciano, A. Guerra-Contreras, S. Lagunas-Rivera, *Org. Chem. Front.* **2022**, *9*, 2856–2888.
[30] B. Bartolomei, G. Gentile, C. Rosso, G. Filippini, M. Prato, *Chem. A Euro. J.* **2021**, *27*, 16062–16070.
[31] Y. Jia, J. Meng, D. Hu, H. Kang, X. Jiang, *Org. Chem. Front.* **2023**, *10*, 2688–2694.
[32] W. D. Castro-Godoy, L. C. Schmidt, D. Flores-Oña, J. Pérez-Prieto, R. E. Galian, J. E. Argüello, *J. Org. Chem.* **2023**, *88*, 6489–6497.
[33] M. H. Muhammad, X.-L. Chen, Y. Liu, T. Shi, Y. Peng, L. Qu, B. Yu, *ACS Sust. Chem. Eng.* **2020**, *8*, 2682–2687.
[34] L. Hao, G. Ding, D. A. Deming, Q. Zhang, *Eur. J. Org. Chem.* **2019**, *2019*, 7307–7321.
[35] Y. Chen, J. Hu, A. Ding, *RSC Adv.* **2020**, *10*, 10661–10665.
[36] K. Yu, H. Zhang, Y. Sheng, Y. Zhu, *Tetrahedron Lett.* **2020**, *61*, 152010–152015.
[37] X. Dong, H. Hao, F. Zhang, X. Lang, *Appl. Catal. B: Env.* **2022**, *309*, 121210–121220.
[38] A. Paul, D. Chatterjee, Rajkamal, T. Halder, S. Banerjee, S. Yadav, *Tetrahedron Lett.* **2015**, *56*, 2496–2499.
[39] M. M. Elsutohy, A. Selo, V. M. Chauhan, S. J. B. Tendler, J. W. Aylott, *RSC Advances* **2018**, *8*, 35840–35848.
[40] S. R. Manne, O. Luna, G. A. Acosta, M. Royo, A. El-Faham, G. Orosz, B. G. De La Torre, F. Albericio, *Org. Lett.* **2021**, *23*, 6900–6904.
[41] Y. Chen, J. Hu, A. Ding, *RSC Adv.* **2020**, *10*, 7927–7932.

[42] E. Albiter, S. Alfaro, M. A. Valenzuela, *Photochem. Photobiol. Sci.* **2015**, *14*, 597–602.
[43] J. Zhao, D. Wu, W. Y. Hernández, W.-J. Zhou, M. Capron, V. V. Ordomsky, *Appl. Catal., A* **2020**, *590*, 117277–117285.
[44] A. I. Carrillo, A. Elhage, M. L. Marin, A. E. Lanterna, *Chem. Eur. J.* **2019**, *25*, 14928–14934.
[45] N. Epelde-Elezcano, R. Prieto-Montero, V. Martínez-Martínez, M. J. Ortiz, A. Prieto-Castañeda, E. Peña-Cabrera, J. L. Belmonte-Vázquez, I. López-Arbeloa, R. Brown, S. Lacombe, *Phys. Chem. Chem. Phys.* **2017**, *19*, 13746–13755.
[46] K. I. Matsui Takafumi; Yamaguchi, Tomoaki; Yamaguchi, Eiji; Tada, Norihiro; Miura, Tsuyoshi; Itoh, Akichika, *Synlett* **2014**, *25*, 2613–2616.
[47] T. Hoshi, J. Okubo, Y. Sakaguchi, M. Kobayashi, H. Inoue, *Ber Bunsenges Phys Chem* **1989**, *93*, 800–805.
[48] Y. Shimada, K. Hattori, N. Tada, T. Miura, A. Itoh, *Synthesis* **2013**, *45*, 2684–2688.
[49] *Fluorescence quenching experiment of AQ with 2-PrOH was performed, see information support (section 5)*
[50] H. G. Kuivila, *J. Am. Chem. Soc.* **1955**, *77*, 4014–4016.
[51] G. K. S. Prakash, S. Chacko, C. Panja, T. E. Thomas, L. Gurung, G. Rasul, T. Mathew, G. A. Olah, *Adv. Synth. Catal.* **2009**, *351*, 1567–1574.
[52] A. Gogoi, U. Bora, *Synlett* **2012**, *23*, 1079–1081.
[53] L. Cui, S. Furuhashi, Y. Tachikawa, N. Tada, T. Miura, A. Itoh, *Tetrahedron Lett.* **2013**, *54*, 162–165.
[54] R. Lindroth, K. L. Materna, L. Hammarström, C.-J. Wallentin, *ACS Org. Inorg. Au* **2022**, *2*, 427–432.
[55] W. R. Leow, J. Yu, B. Li, B. Hu, W. Li, X., Chen, *Angew. Chem. Int. Ed.* **2018**, *57*, 9780–9784.
[56] I. Kumar, R. Sharma, R. Kumar, R. Kumar, U. Sharma, *Adv. Synth. Cat.* **2018**, *360*, 2013–2019.
[57] E. Jin, S. Fu, H. Hanayama, M. A. Addicoat, W. Wei, Q. Chen, R. Graf, K. Landfester, M. Bonn, K. A. I. Zhang, H. I. Wang, K. Müllen, A. Narita, *Angew. Chem. Int. Ed.* **2022**, *61*, e202114059.
[58] D. Prat, A. Wells, J. Hayler, H. Sneddon, C. R. McElroy, S. Abou-Shehada, P. J. Dunn, *Green Chem.* **2016**, *18*, 288–296.
[59] J. Trébosc; J. W. Wiench; S. Huh; V. S.-Y. Lin; M. Pruski, *J. Am. Chem. Soc.* **2005**, 127, 3057–3068.
[60] I. S. Protsak; Y. M. Morozov; W. Dong; Z. Le; D. Zhang; I. M. Henderson, *Nanoscale Research Lett.* **2019**, *14*, 1–15.
[61] M. D. Morales; A. Infantes-Molina; J. M. Lázaro-Martínez; G. P. Romanelli; L. R. Pizzio; E. Rodríguez-Castellón, *Molecular Catalysis*, **2020**, *485*, 110842 (1–11).

10.1002/chem.202303382

WILEY VCH

RESEARCH ARTICLE

Entry for the Table of Contents

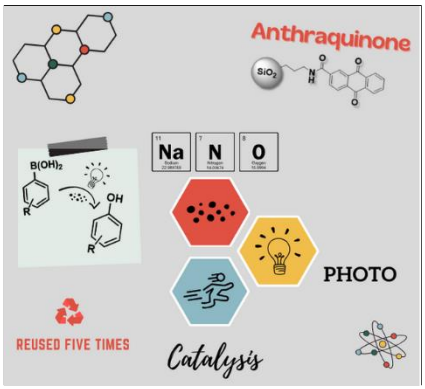

The synthesis and characterization of a heterogeneous photocatalyst based on surface-modified spherical silica nanoparticles with anthraquinone-2-carboxylic acid are presented. The nanomaterial was successfully applied in the aerobic hydroxylation of arylboronic acids to produce phenols in high yields with low catalyst loading and was reused at least five. This heterogeneous system demonstrated promising catalytic activity for conducting organic transformations under sustainable conditions.

Institute and/or researcher Twitter usernames: @infiqcenred